Research Article

Journal of Environmental Nanotechnology

Sol-gel Spin-Coated Si_3N_4 Thin Film Coated on Glass Substrate for Anti-reflection Coating Applications

S. Saravanan[1*], R. S. Dubey[2], P. V. Kumari Chellaboina[3], A. Badarinath[1], K. Padma Pavani[4] and Ch. Rajyalakshmi[4]

[1]Department of Physics (S&H), Swarnandhra College of Engineering and Technology (A), Narsapur, AP, India
[2]JR Research Consulting and Solutions, Nagpur, MH, India
[3]Department of CSE, Swarnandhra College of Engineering and Technology (A), Narsapur, AP, India
[4]Department of Basic Science, Vishnu Institute of Technology, Bhimavaram, AP, India
Received: 11.04.2026 Accepted: 06.05.2026 Published: 30.06.2026
*shasa86@gmail.com

ABSTRACT

Silicon nitride (Si_3N_4) is a ceramic material which is thermodynamically stable with high temperature environment. Silicon nitride thin films find widespread scientific use in solar cells, micro and nano fabrication, antireflection coating (ARC), etc. In this work, Si_3N_4 thin film was deposited on the glass substrate using sol-gel synthesis and spin-coater deposition techniques for anti-reflection coating. The as-deposited thin film was annealed at 500°Cfor its stable structural and optical properties. UV-visible reflectance spectrum revealed the maximum reflectance of 9.26% at a central wavelength of 805 nm, and XRD confirmed the α-Si_3N_4 phase with a crystallite size of 33 nm. The FTIR transmittance spectrum indicated the functional groups of the Si_3N_4 thin film such as low intensity of Si–N characteristic peaks, suggesting minimal nitride content, while the EDS spectrum confirmed the presence of the primary elements Si and N. The topography and roughness of the Si_3N_4 thin film were investigated using AFM, and the average grain size was calculated as 1.8 nm.

Keywords: Si_3N_4; Thin film; Sol-gel synthesis; Spin-coating; Anti-reflection coating.

1. INTRODUCTION

Dielectric thin films are in high demand due to their potential applications in various fields such as LED, solar cells, sensors, micro- and opto-electronic devices. The significant dielectric films are titanium dioxide (TiO_2), silicon dioxide (SiO_2), zinc oxide (ZnO), zirconium oxide (ZrO), and silicon nitride (Si_3N_4) (Nam *et al.* 2024; Nosidlak *et al.* 2023; Dubey and Saravanan, 2022). Among these, Si_3N_4 is one of the most remarkable dielectric materials for their promising applications in integrated circuits and opto-electronic devices. Si_3N_4 thin filmsare fabricated by plasma-enhanced chemical vapor deposition (PECVD), micro-pressure CVD, radio frequency magnetron sputtering, low-pressure CVD, atmospheric pressure CVD, and hot wire CVD (Geetha *et al.* 2025; Merabet *et al.* 2021; Kaloyeros *et al.* 2017; De Luca *et al.* 2021; Alpuim *et al.* 2009). During the experimental process, the properties of the materials can be optimized by adjusting parameters such as deposition time, deposition temperature, calcination temperature, pressure, reactant flow rate, substrates, etc. (Bakardjieva *et al.* 2005) studied the effect of rapid thermally annealed (800, 1000, 1200, and 1400°C) silicon nitride thin films, which were prepared by micro-pressure CVD and plasma-enhanced CVD techniques. The FTIR spectra showed that the Si–N characteristic peak shifted towards higher frequencies with increasing annealing temperature. The effects of rapid thermal annealing treatment on IR peaks, etch rate, dielectric strength, fixed charge density, and hysteresis were examined. (Dubey *et al.* 2017) investigated SiO_2/Si_3N_4 multilayer thin films for solar cell applications using chemical vapor deposition and rigorous coupled wave analysis (RCWA). The fabricated thin films (Si_3N_4/Si and SiO_2/Si) have been studied for thickness and refractive index by ellipsometry. (Thallapalli *et al.* 2016) fabricated Si_3N_4 and boron nitride (BN) composites using the gel casting method. They studied the effect of concentrations of polyethyleneimine and pH on the Si_3N_4-BN particles. The XRD confirmed the α-Si_3N_4, β-Si_3N_4, and BN phases, and SEM images revealed the homogeneous or uniform microstructure. Further, the fracture toughness (2.5 × 5 × 30 mm) and notch length (2.5 mm) were investigated by a single-edge notched beam method. (Meziani *et al.* 2016) investigated the compositional analysis of silicon nitride (SiN_x:H/mc-Si) and silicon oxide (SiO_2/mc-Si) thin films fabricated by PECVD method and thermally oxidized with dry oxygen at ambient atmospheric temperature at 950°C. They demonstrated the existence of silicon and nitrogen elements by EDX spectroscopy. They concluded that the

ratio between N and Si decreased with annealing temperature. (Gan *et al.* 2018) studied the material, structural and mechanical properties of Si_3N_4 and SiO_xN_y thin films prepared by PECVD method. The results revealed mixed composition of amorphous and crystalline Si_3N_4 phases. (Saravanan and Dubey, 2020) analyzed ultrathin film crystalline silicon solar cells using the RCWA method. They proposed a solar cell with the integration of a 70 nm-thick Si_3N_4 antireflection coating, ITO/Al dual nano gratings, distributed Bragg reflectors (SiO_2/Si), and an aluminum substrate. The highest current density of 25.54 mA/cm^2 was achieved by ultrathin-film crystalline silicon solar cells.

In the proposed work, sol-gel synthesized Si_3N_4 thin film was spin coated on glass substrate. These thin film can be integrated in thin film solar cells as anti-reflection coating (ARC) layers.

2. EXPERIMENTAL APPROACH

Table 1. The list of materials used for the synthesis of Si_3N_4 solution

Chemicals	Formula	Mol. Weight(g/mol)
Hexamethyldisiloxane (HMDSO, >98% purity)	$C_6H_{18}OSi_2$	162.38
Ethanol (99.9%)	C_2H_5OH	46.07
Acetic acid (99.9%)	CH_3COOH	60.052
Liquid ammonia (99%)	NH_3	17.031

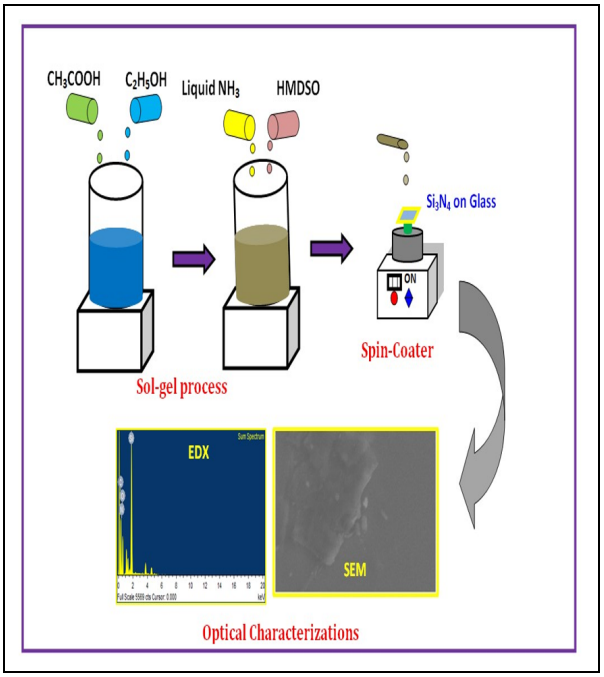


Fig. 1: Schematic diagram of sol-gel synthesis process of Si_3N_4 thin film

The starting source materials for the preparation of silicon nitride thin film are shown in Table 1. Hexamethyldisiloxane(HMDSO) and liquid ammonia are precursor solutions. Ethanol acts as a solvent and aids in controlling the hydrolysis and condensation reactions of the precursor solutions. Acetic acid serves as a catalyst for the hydrolysis of metal alkoxide. In addition, it helps control the pH of the solution and prevents premature gelation.

2.1 The Sol-gel Synthesis and Spin-coating

The schematic diagram is showing the preparation of Si_3N_4 thin film as depicted in Fig. 1.A sol–gel process was employed for the preparation of silicon nitride thin film. Initially, 10 mL of acetic acid was added to 10 mL of ethanol and the solution was stirred continuously for 5 minutes at room temperature using a magnetic stirrer. Then, 5 mL of HMDSO precursor was introduced and mixed thoroughly, followed by the addition of 10 mL of liquid ammonia. In this process, HMDSO and liquid ammonia served as the silicon and nitrogen sources, respectively. The resulting solution was further stirred continuously for 2 hours at room temperature to ensure homogeneity. A transparent, low-viscosity solution was obtained and used for thin film deposition on ultrasonically cleaned glass substrates via the spin coating technique. Each coating was performed at 3000 rpm for 30 seconds. The deposited films were then calcined at 500°C for 1 hour. A total of four coating cycles were carried out to obtain multilayer thin films on the glass substrates.

2.2 Characterization Techniques

The calcined Si_3N_4 thin film was characterized to evaluate its structural, morphological, functional, and elemental properties. X-ray diffraction (XRD; X'Pert Pro, Paralytical, Netherlands) was used to analyze the crystal structure. Fourier transform infrared spectroscopy (FTIR; Spectrum 2, PerkinElmer, USA) and Raman spectroscopy (785 nm excitation, micro-Raman system) were employed to study the bonding and vibrational characteristics. The optical properties were examined using a UV–visible spectrophotometer (UV-1800, Shimadzu, Japan). Surface morphology and roughness were analyzed using atomic force microscopy (AFM; Bruker and Agilent Technologies 5500, USA). Elemental composition was determined using energy-dispersive X-ray spectroscopy (EDS; APEX, Germany).

3. RESULTS AND DISCUSSION

3.1 UV-Visible Spectroscopy (UV-Vis)

The reflectance spectrum of Si_3N_4 thin film measured in the range 300 to 1100 nmis shown in Fig. 2. The maximum reflectance of 9.26% was observed at 805 nm, indicating potential suitability for optoelectronic

applications such as anti-reflection coatings in thin-film solar cells. In addition, the reflectance of the thin film decreased in the longer wavelength region (900–1100 nm). This behavior can be attributed to the decrease in the refractive index of Si3N4with increasing wavelength, which leads to reduced reflection and enhanced transmission. These optical properties endorse the better anti-reflection coating (ARC) properties, which play a major role in photovoltaic (PV) technology to trap the light particles (photons) within the absorber (or active) region. The ARC properties are influenced by the surface roughness of the prepared thin film.

3.2 X-Ray Diffraction

The XRD pattern (Fig. 3(a)) of the Si_3N_4 thin film calcined at 500°Cwas recorded from 10 to 80° with a step size of 0.001 (Ω=2θ) and a relative intensity of 100% The XRD peaks show three major peaks at 2θ = 26, 38, and 48.66°. These XRD diffraction peaks are well matched with the JCPDS card 73–1210 confirming the α-Si_3N_4 structure (Gong-Yi *et al.* 2008). A prominent X-ray diffraction (XRD) peak was observed at approximately 26° corresponding to the (201) plane. This peak exhibited a full width at half maximum (FWHM) of 0.2448° (2θ) and a peak intensity of 184.68 counts. According to the phase diagrams, this major peak was assigned to α-Si3N4(Yang *et al.* 2013). The XRD pattern corresponds to the α-Si3N4 phase with a hexagonal structure confirmed the plane (211) at 38°, as reported by (Hirohata *et al.* 1994) and (Bugaev *et al.* 2012). Using Debye Scherrer's formula,

$$D = \frac{0.9\lambda}{B\cos\theta} \quad \ldots (1)$$

where 'B' is the full width at half maximum (FWHM), 0.89 is the constant number (K), λ is the X-ray wavelength (Cu K_α radiation, 1.5406) and θ is the Bragg angle. The crystallite size was calculated as 33 nm.

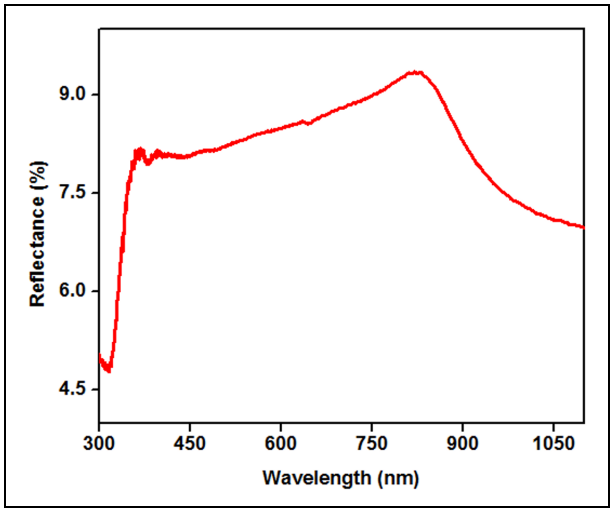


Fig. 2: UV-Visible reflectance of Si_3N_4 thin film

Table 2. Crystalline quality of synthesized Si_3N_4 thin films

S. No.	Sample	Crystalline Quality	Reference
1	Si_3N_4	Hexagonal (uniformly oriented)	(Acosta-Enriquez *et al.* 2016)
2	Si_3N_4	Hexagonal (uniformly oriented)	(Kadhim *et al.* 2017)
3	Si_3N_4	Grain size (21.8- 22.9 nm)	(Beliaev *et al.* 2022)
4	Si_3N_4	Hexagonal with crystallite size 26-30 nm	(Torchynska *et al.* 2015)
5	Si_xN_{1-x}	Single crystalline film and Grain size (21.3-36.9 nm)	(Anber *et al.* 2018)

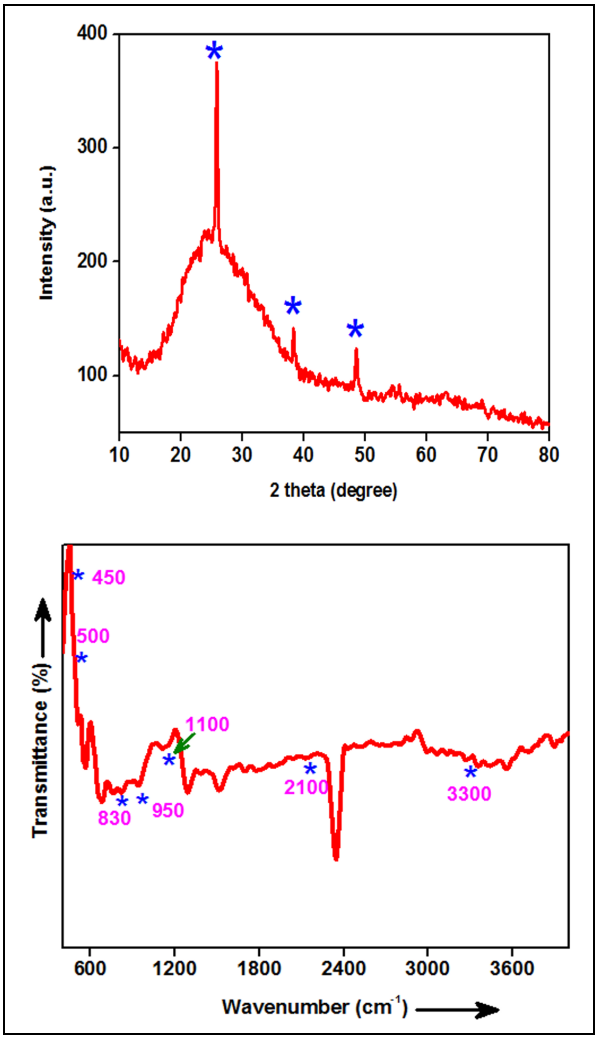


Fig. 3: XRD pattern of sol-gel synthesized Si_3N_4 thin film (a) and FTIR Spectrum (b)

The literature survey of the crystalline quality (defects, orientation, phase, grain size, etc.) of the Si_3N_4 thin films is shown in Table 2. These reported XRD patterns revealed the high quality of the crystals produced, confirming their sharp and intense diffraction peaks. Also, the lower-quality Si_3N_4 crystals may

contribute to the broader or weaker diffraction peaks. Further, to confirm the presence of Si_3N_4, the prepared samples were analyzed by FTIR, Raman, AFM, and EDS spectra.

3.3 FTIR Spectrum

Fig.3(b) depicts the FTIR transmittance (resolution of 16 cm^{-1}) spectrum of Si_3N_4 film recorded in the wavenumber region of 4000 to 400 cm^{-1}.The vibrational modes at 3300 and 2100 cm^{-1} are assigned as N-H and Si-H (Gan *et al.* 2018; Bugaev *et al.* 2012).The IR spectrum of Si_3N_4 shows peaks related to Si-N vibration centered at around 800 and 500 cm^{-1}, respectively. The strong peaks appeared at ~830 and 950 cm^{-1}, which are attributed to the valence oscillation of Si-N bonds. (Hirohata *et al.* 1994) reported broader peaks from 600 to 1200 cm^{-1}, with a peak at 840 cm^{-1}, corresponding to the presence of Si-N symmetric stretching vibration. A weak absorption peak was noticed from 451 to 500 cm^{-1} due to the deformation oscillations of Si-N-Si and N-Si-N as reported by various literature studies (Nam *et al.* 2024; Merabet *et al.* 2021; Yang *et al.* 2013; Hirohata *et al.* 1994). Further, the formation of nitrogen (-NH) vibration modes confirming at 1150 cm^{-1}(Hirohata *et al.* 1994; Bugaev *et al.* 2012). Similarly, (Meziani *et al.* 2016) confirmed the decreased Si/N ratio concentration due to the increase in calcinations temperature. When comparing the formation of Si_3N_4 thin films, preventing oxygen molecules by forming Si-H and N-H bonding is reported by (Gan *et al.* 2018). However, the oxygen element is present due to the calcinations atmosphere (or) during the sample testing as depicted in Fig. 6.

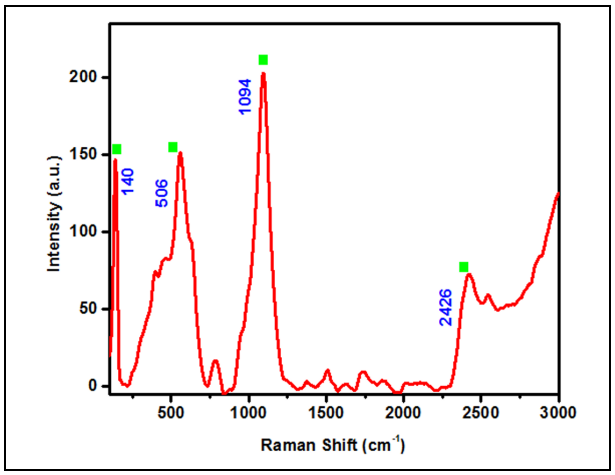


Fig. 4: Raman spectrum of prepared Si_3N_4 thin film

3.4 Raman Spectrum Study

Fig.4shows the Raman spectrum of the thin film.The most intense Raman bands were noticed at 140, 506, 1094, and 2426 cm^{-1}, attributed to the vibrational modes of the lattice. These modes are assigned to the internal modes of the thin film. The sharp peak position and the width of the peak strongly depend on the thin film thickness and structure. Accordingly, the dispersion of the localized modes is changing (Hirohata *et al.* 1994). The peaks at 140, 506, and 1094 cm^{-1} confirm the presence of α-Si_3N_4, as reported by various literature data (Kang *et al.* 2014).The broader peak observed around 506 cm^{-1}corresponds to the presence of Si-N stretching mode and the other peaks corresponding to α-Si_3N_4.This feature is associated with structural disorder, where some silicon atoms are replaced or coordinated with nitrogen atoms (Debieu *et al.* 2013; Ahmed *et al.* 2013; Volodin *et al.* 1998).

3.5 Atomic Force Microscopy Study

The smooth and homogenous surface of the thin film was confirmed by AFM topography images, as shown in Fig.5.

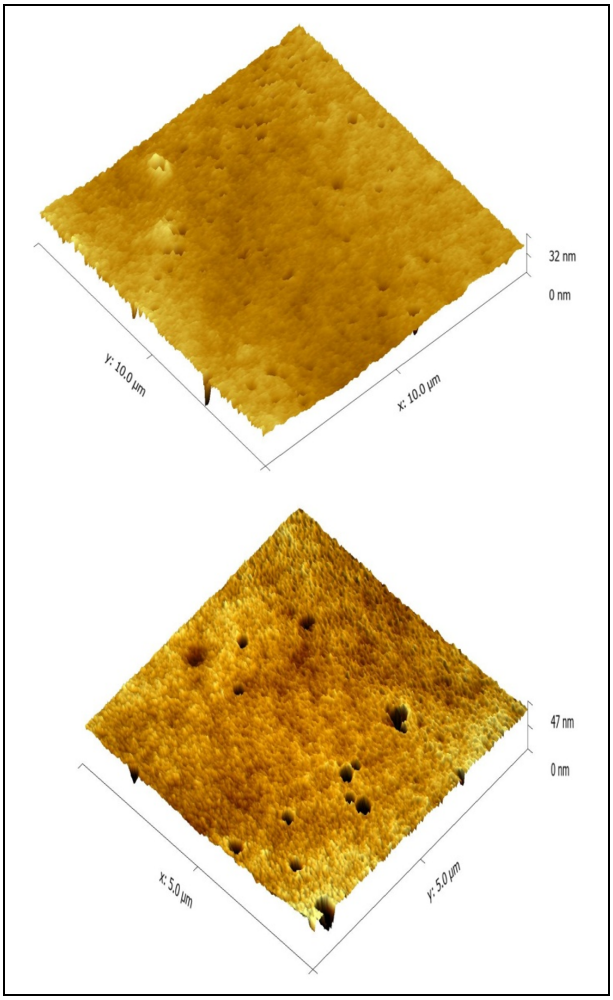


Fig.5: The AFM image of Si_3N_4 thin films

The AFM analysis was performed at two different surface regions of the sample of Si_3N_4 thin film on glass substrates (length and width = 2 × 2 cm). From Fig. 5(a)-(b), the thickness of the thin film was observed

as 47 and 32 nm in two different regions. These smooth surfaces of Si_3N_4 thin film have a few small holes (like porous ones) due to defects in the sample, which will be optimized.

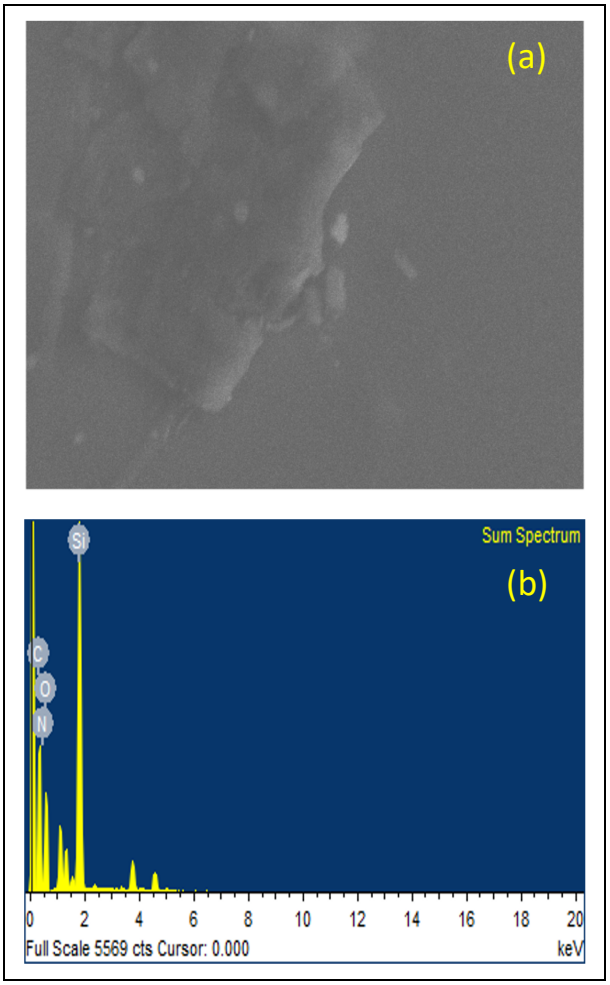


Fig. 6: The electronic image (a) and corresponding EDS spectrum and (b) of Si_3N_4

Furthermore, the average grain size of the sample was calculated as 1.8 nm. Also, the analysis of the grain boundaries of various locations tested showed similar results.

3.6 Energy Dispersive X-ray Spectroscopy Study

The elemental analysis of the Si_3N_4 thin film was carried out by EDS spectroscopy. The SEM image confirmed the formation of a smooth, thin film surface on the glass substrate, as depicted in Fig. 6 (a). The elemental spectrum depicted the typical Si_3N_4 result of the primary elements of Si and N (Fig. 6(b)) (Gong-Yi *et al.* 2008). Also presented are the various impurities of oxygen (O) and carbon (C) peaks associated with the muffle furnace during the calcinations (Dubey *et al.* 2017). The atomic weight percentages of the elements in the sample are given in Table 3. Here, the peak of nitrogen shows a reduced weight percentage due to the calcination's temperature. The formation of Si_3N_4 thin films is significantly influenced by the calcination's temperature. Higher calcinations temperature generally leads to enhanced film densification, crystallinity, and stoichiometry, resulting in improved mechanical, electrical, and optical properties of the thin films. Additionally, it can promote the removal of organic residuals, improve reaction kinetics, and reduce defects in the film structure.

Table 3. The list of elements presents in Si_3N_4 thin film

S.No.	Element(K)	Weight (%)	Atomic (%)
1	Si	14.04	7.17
2	N	3.87	3.96
3	O	30.71	27.52
4	C	51.39	61.35

Table 4. The reported sol-gel synthesis method for the preparation of Si_3N_4 thin film

S.No.	Thin Film	Preparation Methods	Ref.
1	TiO_2/Si_3N_4	sol-gel spin-coating	(Nam *et al.* 2024)
2	Si_3N_4	sol-gel	(Andrew,2016)
3	Si_3N_4	sol-gel dip-coating	(Shereen *et al.* 2011)

However, excessively high temperatures can also lead to film degradation, increased surface roughness, and stress-induced cracking. Therefore, optimizing the calcinations temperature is crucial for achieving the desired film properties (Volodin *et al.* 1998). Some of the reported works on Si_3N_4 thin film based on the sol-gel synthesis method are given in Table 4.

4. CONCLUSION

In this work, the silicon nitride (Si_3N_4) thin films were prepared using sol-gel spin-coating deposition technique. Four thin film layers were deposited on the glass substrate, which was calcinated at 500°C. The thin film was characterized for its optical, structural, functional groups, topographical, and elemental properties by various characterization techniques such as UV-visible spectroscopy, FTIR, XRD, Raman, AFM, and EDX spectroscopy. The UV-Vis reflectance spectrum showed low reflection of 9.26% at 805 nm (λ). The FTIR transmittance spectrum exhibited various peaks corresponding to characteristic functional groups related to the Si_3N_4. The XRD diffraction pattern revealed the presence of α-Si_3N_4 phases at (201), (211) with hexagonal structures. Further, the AFM depicted the topography and smooth thin film surface of $Si_3N_4$with porous nature with an average grain size of 1.8 nm. The EDS spectrum showedSi and N as the primary elements

confirming the successful preparation of Si_3N_4 thin film. In future, optimization processes will be carried out for better ARC in solar cells with green synthesis method.

ACKNOWLEDGEMENT

The authors would like to express their sincere gratitude to the Principal and Management of Swarnandhra College of Engineering and Technology (A), Narsapur, West Godavari (AP), India providing the necessary resources and infrastructure to conduct this research.

FUNDING

This research received no specific grant from any funding agency in the public, commercial, or not-for-profit sectors.

CONFLICTS OF INTEREST

The authors declare that there is no conflict of interest.

COPYRIGHT

This article is an open-access article distributed under the terms and conditions of the Creative Commons Attribution (CC BY) license (http://creativecommons.org/licenses/by/4.0/).



REFERENCES

Acosta-Enriquez, E. B., Acosta-Enriquez, M. C., Castillo-Ortega, R., Zayas, M. A. E. and Pech-Canul M. I., Nanostructured Fibers of A-Si_3N_4 Deposited By HYSY-CVD, *Digest J. Nanomater. Biostruct.,* 11(2), 601-605 (2016). https://chalcogen.ro/601_AcostaE.pdf

Ahmed, N., Singh, C. B., Bhattacharya, S., Dhara, S., Balaji, B. P., Raman and FTIR studies on PECVD ammonia-free amorphous silicon nitride thin films for solar cell applications, *Energy,* 1-4 (2013). https://doi.org/10.1155/2013/837676

Alpuim, A., Goncalves, L. M., Marins, E. S., Viseu, T. M. R., Ferdov, S. and Bouree, J. E., Deposition of silicon nitride thin films by hot-wire CVD at 100°C and 250°C, *Thin Solid Films,* 517 (12), 3503-3506 (2009). https://doi.org/10.1016/j.tsf.2009.01.077

Anber, A. A. and Kadhim, F. J., Preparation of nanostructured Si_xN_{1-x} thin films by DC reactive magnetron sputtering for tribology applications, *Silicon,* 10(3), 821-824 (2018). https://doi.org/10.1007/s12633-016-9535-4

Andrew, L. H., Synthesis and processing of silicon nitride and related materials using preceramic polymer and non-oxide sol-gel approaches, *Coordinat. Chem. Rev.,* 323, 120-137 (2016). https://doi.org/10.1016/j.ccr.2016.05.009

Bakardjieva, V., Beshkov, G., Vitanov, P. and Alexieva, Z., Effect of rapid thermal annealing on the properties of PCVD and PECVD silicon nitride thin films, *J. Optoelectron. Adv. Mater.,* 7 (1), 377-380 (2005). https://old.joam.inoe.ro/arhiva/pdf7_1/Bakardjieva.pdf

Beliaev, L. Y., Shkondin, E., Lavrinenko, A. V. and Takayama, O., Optical, structural and composition properties of silicon nitride films deposited by reactive radio-frequency sputtering, low pressure and plasma-enhanced chemical vapor deposition, *Thin solid films,* 763, 139568 (2022). https://doi.org/10.1016/j.tsf.2022.139568

Bugaev, K. O., Zelenina, A. A. and Volodin, V. A., Vibrational spectroscopy of chemical species in silicon and silicon-rich nitride thin films, *Int. J. Spectros.,* 2012,1-5 (2012). https://doi.org/10.1155/2012/281851

De Luca, D., Di Gennaro, E., De Maio, D., D'Alessandro, C., Antonio, C., Musto, M., Can, K., Andreone, A., Rosalba, F., Valentina, D. M., Mario, I. and Russo, R., Tuning silicon nitride refractive index through ratio-frequency sputtering power, *Thin Solid Films,* 737 (1),138951 (2021). https://doi.org/10.1016/j.tsf.2021.138951

Debieu, O., Nalini, R. P., Cardin, J., Portier, X., Perriere, J. and Gourbilleau, F., Structural and optical characterization of pure Si-rich nitride thin films, *Nanoscale Res. Lett.,* 8(1), 31(2013). https://doi.org/10.1186/1556-276X-8-31

Dubey, R. S., Jhansirani, K. and Singh, S., Investigation of solar cell performance using multilayer thin film structure (SiO_2/Si_3N_4) and grating, *Res. Phy.,* 7, 77-81 (2017). https://doi.org/10.1016/j.rinp.2016.11.065

Dubey, R. S. and Saravanan, S., Optical study of sol-gel spin-coating TiO_2/Si_3N_4 multilayers on glass substrates, *Rasayan J. Chem.,* 15(4), 2304-2309 (2022). https://doi.org/10.31788/RJC.2022.1547077

Gan, Z., Wang, C. and Chen, Z., Material structures and mechanical properties of silicon nitride and silicon oxynitride thin films deposited by plasma enhanced chemical vapor deposition, *Surf.,* 1(1), 59-72 (2018). https://doi.org/10.3390/surfaces1010006

Geetha, M., Dubey, R. S. and Saravanan, S., Investigation of anti-reflective silicon nitride (Si_3N_4) thin film: A CVD techniques Opto-electronics and advanced Materials, 27(7-8), 326-333 (2025).

Gong-Yi, L., Xiao, D. L., Hao, W. and Zhong, Q. L., Long silicon nitride nanowires synthesized in a simple route, *Appl. Phys. A,* 93(2), 471-475 (2008). https://doi.org/10.1007/s00339-008-4808-4

Hirohata, Y., Shimamoto, N., Hino, T., Yamashima, T. and Yabe, K., Properties of silicon nitride films prepared by magnetron sputtering, *Thin Solid Films,* 253(1-2), 425-429 (1994). https://doi.org/10.1016/0040-6090(94)90360-3

Kadhim, F. J., Khalaf, M. K. and Hammadi, O. A., Preparation and characterization of silicon nitride nanostructures prepared by DC reactive sputtering technique with novel design of closed-field unbalanced dual magnetron assembly, *IRAQI J. Appl. Phy.,* 13(3), 3-12 (2017).

Kaloyeros, A. E., Pan, Y., Goff, J. and Arkles, B., Review-Silicon nitride and silicon nitride-rich thin film technologies: Trends in deposition techniques and related applications, *ECS J. Sol. State Sci. Technol.,* 6(10), 691-714(2017). https://doi.org/10.1149/2.0011710jss

Kang, S., Lee, H. W., Hong, M. P. and Kwang-Ho, K., Characteristics of room temperature silicon nitride deposited by internal inductively coupled plasma chemical vapor deposition, *J. Nanosci. Nanotechnol.,* 14(8), 6189-6195 (2014). https://doi.org/10.1166/jnn.2014.8816

Merabet, H., Luna, Y. D., Mohamed, K. and Bensalah, N., Fabrication of Si_3N_4@Si@Cu thin films by RF sputtering as high energy anode material for Li-Ion Batteries, *Mater.,* 14(11), 2824 (2021). https://doi.org/10.3390/ma14112824

Meziani, S., Moussi, A., Mahiou, L. and Outemzabet, R., Compositional analysis of silicon oxide/silicon nitride thin films, *Mater. Sci. Poland,* 34 (2), 315-321 (2016). https://doi.org/10.1515/msp-2016-0057

Nam, M., Lee, S., Jeong, H., Yoon, A. Park, J. S. and Jeon, W., Optimizing the crystallinity of a ZrO_2 thin film insulator for InGaZnO –based Metal –Insulator-Semiconductor capacities, *Adv. Mater. Interf.,* 11(11), 2300883 (2024). https://doi.org/10.1002/admi.202300883

Nosidlak, N., Jaglarz, J., Vallati, A., Dulian, P., Maria, J. S., Sylwia, G., Aleksandra, S., Lukasz, W., Witkowski, B. S. and Marek, G., The optical properties of thin film alloys of ZnO, TiO_2 and ZrO_2 with Al_2O_3 synthesized using atomic layer deposition, *Coatings,* 13(11), 1872 (2023). https://doi.org/10.3390/coatings13111872

Saravanan, S. and Dubey, R. S., One-dimensional photonic crystals (Si/SiO_2) for ultrathin film crystalline silicon solar cells, *Nanosyst. Phy., Chem., Math.,* 11 (2), 189-194 (2020). https://doi.org/10.17586/2220-8054-2020-11-2-189-194

Shereen, H., Hector, A. L. and Kalaji, A., Sol-gel processing of silicon nitride films from $Si(NHMe_4)$ and ammonia, *J. Mater. Chem.,* 21(17), 6370-6374 (2011). https://doi.org/10.1039/C1JM10127G

Thallapalli, N., Kishore, K. K. and Rao, C. S. P., Preparation and characterization of Si_3N_4-BN Ceramic composites by Gelcasting, *Mater. Sci. Res. Ind.,* 13(1), 28-33 (2016). http://dx.doi.org/10.13005/msri/130105

Torchynska, T. V., Casas, E. J. L., Khomenkova, L., Hernandez, E. V., Andraca, A. J. A. and Slaoui, A., Structural and light emitting properties of silicon-rich silicon nitride films grown by plasma enhanced-chemical vapor deposition, *Mater. Sci. Semicond. Proce.,* 37, 46-50 (2015). https://doi.org/10.1016/j.mssp.2015.01.018

Volodin, V. A., Efremov, M. D., Gritsenko, V. A. and Kochubei, S. A., Raman study of silicon nanocrystals formed in SiNx films by excimer laser or thermal annealing, *Appl. Phy. Lett.,* 73(9), 1212–1214 (1998). https://doi.org/10.1063/1.122130

Yang, W. W., Inada, M., Tanaka, Y., Enomoto, N. and Hojo, J., Fabrication of translucent silicon nitride ceramics with various sintering aids, *Int. J. Nanotechnol.,*10 (1/2), 119-125 (2013). https://doi.org/10.1504/IJNT.2013.050888